

Interactions between MHD instabilities in the wall-stabilized high- β plasmas

G. Matsunaga, N. Aiba, K. Shinohara, Y. Sakamoto, M. Takechi, T. Suzuki, N. Asakura, A. Isayama, N. Oyama, M. Yoshida, K. Kamiya, H. Urano, T. Nakano, Y. Kamada and the JT-60 Team

Japan Atomic Energy Agency, Naka 311-0193, Japan

E-mail: matsunaga.go@jaea.go.jp

Abstract. In the JT-60U wall-stabilized high- β_N plasmas, interactions between MHD instabilities have been observed. It is observed that an energetic particle driven wall mode (EWM) triggers an edge localized mode (ELM). When the EWM appears, type-I ELM crashes are synchronized with EWM bursts. The EWM-triggered ELMs have a higher frequency and less energy release than those of usual type-I ELMs. This interaction mainly occurs when the EWM with a large amplitude appears. In the SOL region, several measurements indicate ion losses induced by the EWM. Abrupt ion losses through the edge can increase as local pressure gradient at the pedestal that determines the edge stability. Moreover, another interaction that an EWM-triggered ELM excites marginal resistive wall mode (RWM) is observed. Just after the EWM-triggered ELM, an $n = 1$ distortion appears and decays soon. It is considered that an impact of the induced ELM can excite the marginally stable RWM.

1. Introduction

Toward sustainment of burning high- β_N plasmas, the understanding of MHD events in the high- β_N plasmas is important. Particularly, the high- β plasmas above the no-wall limit, where the resistive wall mode (RWM) limits the achievable β_N , have been exploited based on researches of stabilization mechanisms of the RWM. Note that since in the high- β plasma above the no-wall limit the ideal mode is stabilized by the conducting wall, the plasma is the so-called “wall-stabilized high- β_N plasmas.” The MHD events in this region determine stability, eventually performance of a reactor. Finally, it is preferable to control any MHD event for the steady state high- β_N plasmas. In the JT-60U wall-stabilized high- β_N plasmas, the interactions between MHD instabilities have been observed. Namely, an energetic particle driven mode named “Energetic particle driven wall mode (EWM)” triggers an edge localized mode (ELM); EWM-triggered ELM. The EWM-triggered ELMs have a higher repetition frequency and less energy release compared with usual type-I ELMs. This phenomenon may contribute ELM mitigation control. The details of the EWM have been reported [1, 2]. The EWM seems to be “fishbone-like” burst with frequency chirping down in a few milliseconds, whose time scale can not be explained by thermal plasma dispersion. Its initial frequency is close to the precession frequency of the trapped energetic ions from the perpendicularly injected neutral beams (PERP-NBs). From the results, the EWM is found to be driven by the trapped energetic ions. Similar instability is also observed in the high- β_N plasma on DIII-D [3]. Since the EWM can sometimes induce the RWM despite enough plasma rotation. In this paper, we focus on the EWM-triggered ELM and report the details of this phenomenon.

2. Observation of EWM-triggered ELM

In JT-60U high- β_N plasmas, pedestal stability is limited by type-I ELMs that can induce the energy loss which is $\sim 10\%$ of the pedestal stored energy W_{ped} and $\sim 3\%$ of the total stored energy W_{dia} . It has been observed that an EWM triggers an ELM in ELMy H-mode plasmas with high- β_N . Figure 1 shows an example of high- β_N discharge with $B_t = 1.5$ T, $I_p = 0.9$ MA, $\beta_N \simeq 3.0$ and $q_{95} \simeq 3.3$. In Fig. 1, drops of W_{dia} and spikes in D_α emission correspond to

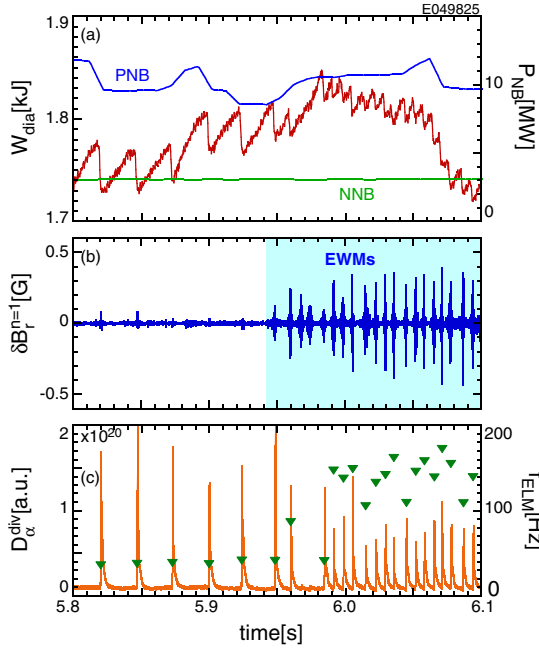


Fig. 1: Observation of EWM-triggered ELM in the wall-stabilized high- β_N plasma. (a) stored energy, NB power, (b) magnetic fluctuation, (c) D_{α} emission at divertor region and ELM repetition frequency.

ELM crashes. Bursts in the magnetic fluctuation in Fig. 1(b) correspond to EWMs. During the appearance of the EWMs at $t = 5.94$ s (highlighted), the ELM behavior is changed. In this phase, each ELM is synchronized with the EWM, suggesting the EWM burst can trigger the ELM. The repetition frequency of the ELM, which is defined as the inverse of the ELM interval, becomes twice or more higher compared with the no-EWM phase. At the same time, the stored energy drop ΔW_{dia} due to an ELM crash became smaller.

Figure 2 shows the ELM frequency versus the normalized ELM energy loss for the type-I ELM (red circles) and the EWM-triggered ELM (blue squares). The energy losses are normalized by the stored energy in the pedestal region; $W_{\text{ped}} = \frac{3}{2}(n_e^{\text{ped}} T_e^{\text{ped}} + n_i^{\text{ped}} T_i^{\text{ped}}) k_B V_p$, where k_B and V_p are the Boltzmann constant and the plasma volume; the subscript 'ped' denotes the values at the pedestal top. During no EWM phase, the normalized energy loss $\Delta W_{\text{dia}}/W_{\text{ped}}$ is $\leq 15\%$. Meanwhile, during the EWM phase, it becomes smaller, thus, $\Delta W_{\text{dia}}/W_{\text{ped}} \leq 8\%$. These behaviors are similar to ELM mitigation. This phenomenon is almost certainly observed when the EWM with a large amplitude appears, as is discussed in the following section.

3. Comparison of Type-I and EWM-triggered ELMs

Waveforms of type-I ELM, EWM-triggered ELM and EWM without ELM trigger (hereafter: EWM alone) are compared. As shown in the left panels in Fig. 3, magnetic fluctuation of a precursor is not clearly observed for type-I ELMs. Since the usual type-I ELM is associated with intermediate or high- n MHD instability at the edge, it is hard to measure magnetic fluctuations of its precursor by the magnetic sensors at the wall. This type-I ELM induced an energy loss of 50 kJ, that is $\sim 13\%$ of W_{ped} . The center panels show waveforms of an EWM-triggered ELM. The EWM is growing until an ELM is triggered, and then the EWM amplitude rapidly decays. As the EWM is decaying, the EWM mode frequency is chirping down. The frequency chirping indicates that the interaction between the EWM and the energetic ions, that

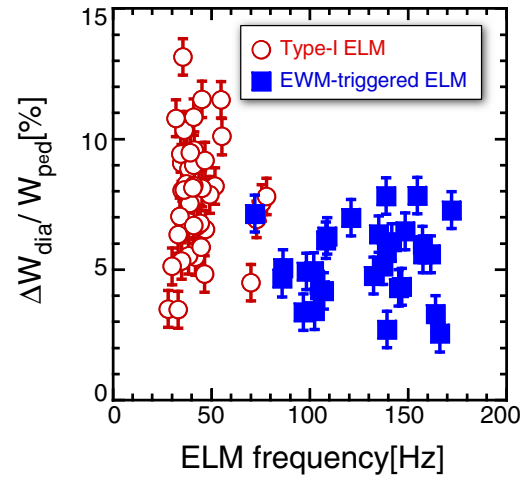


Fig. 2: ELM repetition frequency versus energy loss normalized by W_{ped} of each ELM crash. Red circles and blue squares correspond to Type-I and ELM-triggered ELM, respectively.

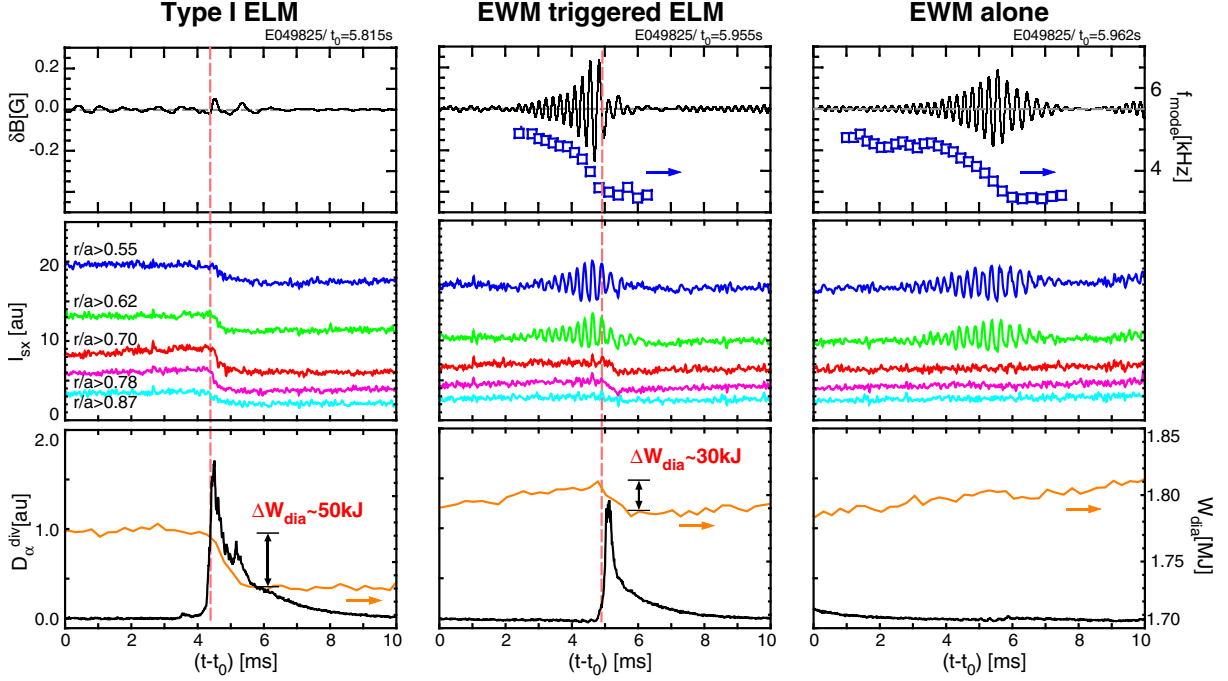


Fig. 3: Comparison among waveforms of (Left) Type-I ELM, (Center) EWM-triggered ELM and (Right) EWM alone. From the top, magnetic fluctuations with mode frequencies, soft X-ray emissions, D_α emissions at divertor region and the total stored energies.

is, redistribution and/or loss of the energetic ions in both velocity space and real space. Soft X-ray emissions indicates crashes at the pedestal region due to the EWM-triggered ELM. This EWM-triggered ELM induces an energy loss of 30 kJ, that is $\sim 5\%$ of W_{ped} less than that of the type-I ELM. After the crash, the EWM mode amplitude decays quickly compared with the EWM alone, suggesting that the driving source of the EWM, that is, energetic ions, is lost by this crash. The right panels show waveforms of EWM alone. The EWM grows and decays, which is thought to be determined by the competition between driving and damping mechanisms related to energetic ion confinement. Although D_α emission at the divertor did not clearly change, an increase of D_α emission in the sight line to the plasma top is observed as mentioned in the following section.

Figure 4 shows time evolutions of waveforms involving both type-I ELM and EWM-triggered ELM. In this time window, EWMs appeared at $t = 5.95$ s after the type-I ELM phase. Radial affected region of the type-I and the EWM-triggered ELM are measured by the electron cyclotron emission (ECE) and estimated by the Abel inverted soft X-ray emissions shown in Figure 5. These are estimated as differences between before and after I_{sx} profiles with a time lag of 2 ms. As for a type-I ELM at $t \simeq 5.90$ s, T_e profile is changed in the region where $r/a \geq 0.6$. On the other hand, the affected region of an EWM-triggered ELM at $t \simeq 5.96$ s is the region where $r/a \geq 0.7$. These results also show that the EWM-triggered ELM is smaller than that of the type-I ELM, consistent with the difference of ΔW_{dia} .

4. Relation between EWM amplitude and ELM trigger

It is observed that the EWM can trigger the ELM, however, it is not always. Thus, whether the EWM can trigger or not depends on the EWM amplitude. Figure 6 shows the relation between the amplitudes δB_r^{max} and the growth rates γ_{EWM} of the EWMs. Here, the amplitude is defined as the maximum value of the envelope of the EWM perturbation; the growth rate

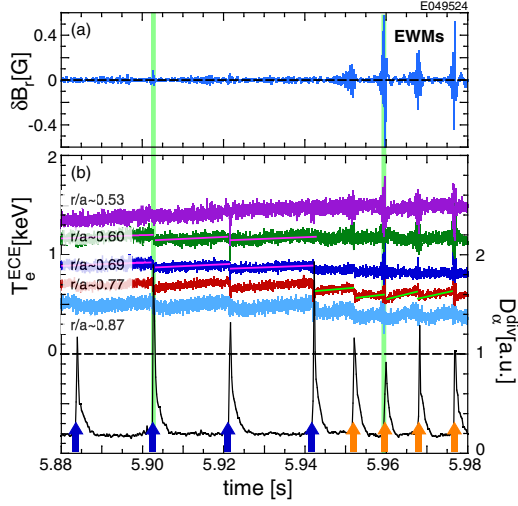


Fig. 4: Time evolutions of waveforms involving both type-I ELM and EWM-triggered ELM. (a) magnetic fluctuation, (b) T_e measured by ECE and D_α emission at the divertor region.

is defined by an exponential curve fitting during the mode growing. This figure shows a clear correlation between δB_r^{\max} and γ_{EWM} . In this figure, red squares and blue circles correspond to the EWM with and without ELM trigger, respectively. The upper right region indicates the EWM with large amplitude and growth rate. The EWM with a large amplitude can almost certainly trigger the ELM. Meanwhile, on the lower left region, the EWM with small amplitude can not trigger the ELM any longer. Figure 7(a) and (b) show typical EWM waveforms with a large and small amplitude, respectively. The large EWM is rapidly grows and then trigger an ELM. The small EWM slowly grow and the amplitude is saturated and then decays. Since the EWM is driven by the energetic ions, the grow and decay are determined by the spatial profile and the distribution in the phase space of the energetic ions. On the middle range in Fig. 6, the EWM with a medium amplitude can not always trigger the ELM. On the phase where the medium EWMs appear, a mixture phenomenon of the type-I ELM and EWM-triggered ELM is observed.

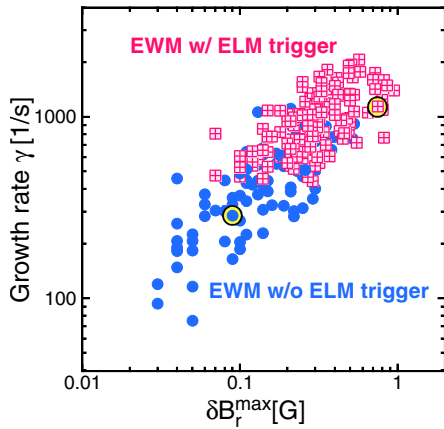


Fig. 6: Maximum amplitudes and growth rates of EWM with (Red squares) and without ELM trigger (blue circles). Circles indicate EWMs that are shown in Fig. 7.

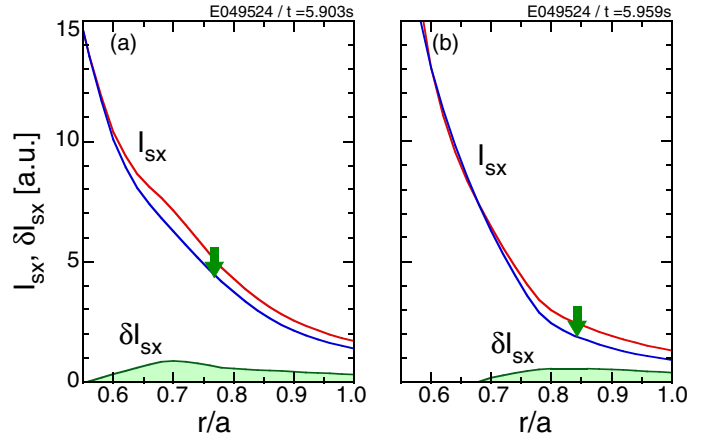


Fig. 5: Affected areas by (a) type-I ELM and (b) EWM-triggered ELM estimated as Abel inverted soft X-ray emissions. RED and blue lines show I_{sx} profiles before and after crashes. Green lines shows differences between before and after profiles.

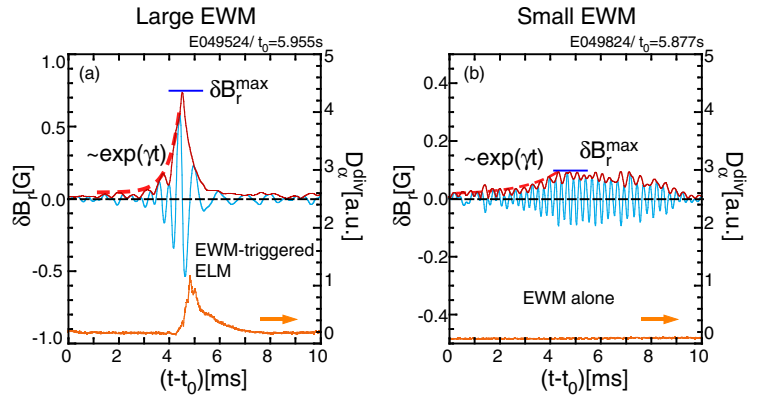


Fig. 7: Example of EWM waveforms with (a) large and (b) small amplitude. Magnetic fluctuation and D_α emission are indicated.

5. SOL behaviors due to EWM

It is observed that interesting correlations between the EWM and the SOL plasma. Figure 8 shows signals in the scrape off layer (SOL) plasma during the EWM alone phase (highlighted). The viewing chords and measured locations of these diagnostics are shown in Fig. 9. These signals are strongly synchronized by the EWM amplitude. The floating potentials are measured by the Langmuir probes on the divertor targets at both the low field side (LFS) and the high field side (HFS). These target probes are located at the ends of the SOL plasma where magnetic field lines go round core plasma as shown in Fig. 9 (red lines). These floating potentials measured on the divertor targets indicate positive spikes synchronized with an EWM amplitude. The increase of the positive spikes are several tens volts. Although the SOL physics is complicated, the observed positive spikes are possible to relate the ion transport from core to SOL plasma by the EWM. Since the EWM has a large amplitude at the LFS, the EWM can interact with the SOL plasma via the expelling the ions from the core plasma. Similar increases are observed in the signals of D_α emission and carbon impurity line (C II) in the sight lines of the plasma top. Note that D_α signal at the plasma top D_α^{top} is clearer than D_α^{div} as for the influence of EWM because signal gain of D_α^{div} is optimized so as to measure large emission due to ELMs. These signals correspond to the recycling of deuterium and the sputtering of carbon impurities caused by the ion impacts to the wall. This observation indicates that an EWM enhances the ion transport, thus, an EWM can expel ions to the wall.

From the view point of the correlation between the EWM amplitude and D_α emission, these events of the type-I ELM, the EWM-triggered ELM and the EWM alone are compared. The D_α emission clearly increases as the EWM occurs. This indicates that the expelled ions due to the EWM increases the recycling at the wall. Namely, the increase of D_α is thought to correspond to the ion losses. Figure 10 shows the dependence of D_α^{top} and EWM amplitude B_{env} . Here, an envelope of the EWM perturbation B_{env} is used as the mode amplitude; an averaged valued

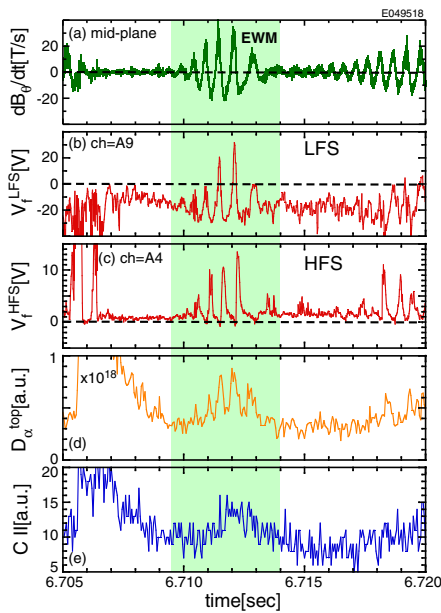


Fig. 8: Synchronized signals with EWM. From the top, (a) magnetic fluctuation, floating potentials at divertor target probes at (b) LFS and (c) HFS, (d) D_α emission and (e) carbon impurity line at the top of plasma.

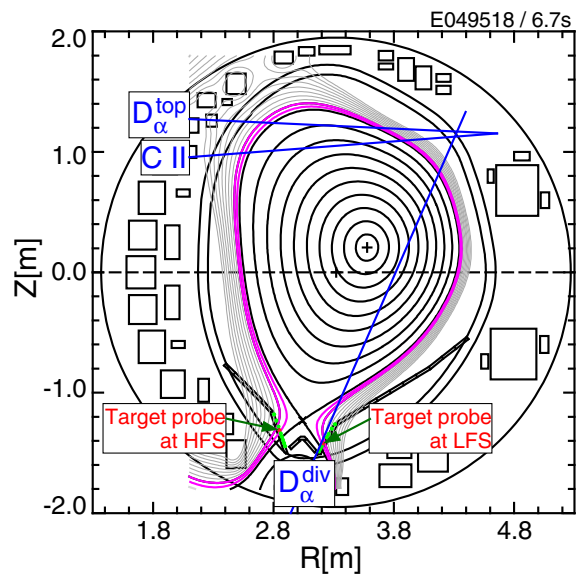


Fig. 9: Sight lines of diagnostics and probe locations with core and SOL plasmas.

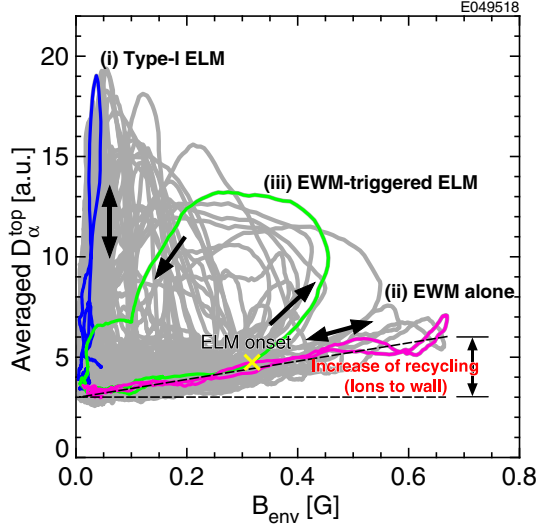


Fig. 10: Trajectories in D_α^{top} and amplitude of enveloped magnetic fluctuation. Colored lines indicate the each trajectory of type-I ELM, EWM-triggered ELM and EWM alone.

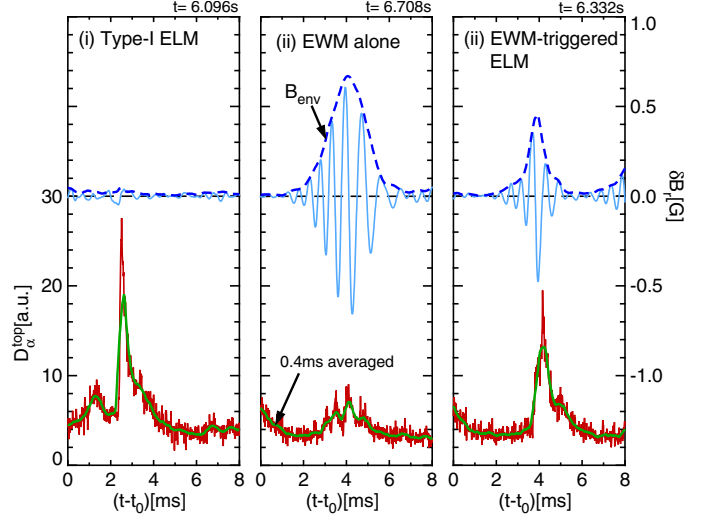


Fig. 11: Comparisons between waveforms between (i) type-I ELM, (ii) EWM alone and (iii) EWM-triggered ELM.

of D_α^{top} is used as for D_α^{top} . The gray lines in $D_\alpha^{\text{top}}-B_{\text{env}}$ diagram indicate the trajectories for a typical discharge of E049518, where the type-I ELM, the EWM-triggered ELM and the EWM alone were observed. Colored lines indicate each trajectory as shown in Fig. 11. First, the type-I ELM independently behaves with respect to B_{env} . Second, the trajectory of the EWM alone has a strong correlation. The D_α^{top} emission increases linearly as the EWM mode amplitude increases. This dependence suggests that the EWM can enhance a recycling in the SOL region indicating ion losses to the wall. Third, as for the EWM-triggered ELM, the trajectory behaves as the same as that of the EWM alone in the early phase. After the ELM onset, D_α^{top} rapidly increases and decays as the EWM amplitude decreases. The decay of the EWM is thought to arise from the losses of energetic ions caused by the ELM crash. The results suggest whether the EWM can trigger an ELM is not determined only by an EWM amplitude (induced ion losses).

In the previous research, it is found the EWM is driven by trapped energetic ions. Actually, the mode frequency of the EWM is chirping down, indicating the EWM affect energetic ions because a time scale of the frequency chirping can not be explained by the thermal plasma dispersion. Moreover, the EWM amplitude also decreases accompanied with the frequency chirping down. These suggest that the EWM induces a transport of “energetic” ions, that is, a redistribution and/or loss. Therefore, it is possible to conclude that the observed ion losses correspond to the “energetic” ion losses.

6. Possible interpretation of EWM-triggered ELM

At first, the obtained results are briefly summarized: (i) an EWM can trigger an ELM; (ii) the repetition frequency of EWM-triggered ELMs is, at least, twice higher than that of type-I ELMs; (iii) an energy release and an affected area of the EWM-triggered ELM are smaller than those of an type-I ELM; (iv) the large EWM can almost certainly trigger the ELM; (v) SOL measurements indicate that ion transport is enhanced by the EWM; (vi) an ELM can not always triggered even by a larger EWM. From these results, the mechanism of EWM-triggered ELM is discussed with the edge stability.

Figure 12 shows an edge stability diagram, $j-\alpha$ diagram, calculated by MARG2D code [4, 5]

based on parameters just before the type-I ELM in the typical discharge (E049350) where type-I ELMs and EWM-triggered ELMs coexist. Here, j and α are an edge current density and the normalized pressure gradient; the edge current density is described as an averaged current density at the pedestal region $\langle j_{\text{ped}} \rangle$ normalized by the averaged current density $\langle j \rangle$. In Fig. 12, there are two stability boundaries of a finite- n and an infinite- n MHD limits. The cross with circle indicates the edge status just before the type-I ELM. It is found that the edge status is close to the finite- n limit. Namely, the type-I ELM occurs as the edge parameters (j, α) reach the finite- n limit. After the type-I ELM crash, both j, α in the edge are lost, resulting in moving the edge status downward lower left in this diagram. In the case of usual type-I ELM, the edge status moves to upper right in the diagram again as W_{ped} is recovering, as is an ELM cycle. In the EWM-triggered ELM case, since the EWM can induce ion losses, the ions can affect as an additional α . With taking into account this effect, the edge status can be shifted close to these boundaries. If this shift is enough to reach to the boundaries, an ELM can be triggered. Since the EWM has an $n = 1$ mode structure, induced ion losses are considered to be localized and rotating toroidally. Thus, EWM induced ion losses are thought to violate the edge stability at the region where losses are the maximum. At the moment, we have interpreted whether an EWM can trigger an ELM is determined by the competition between a distance from the MHD boundary and additional pressure of ion losses due to an EWM.

As discussed in the previous section, if ion loss induced by the EWM is the “energetic” ion loss, the energetic ion loss can effectively act as an additional pressure, because energies of the energetic ions are at least several tens times higher than T_i and T_e at the edge. This means that the energetic ions are effective as additional pressure even with a small amount of energetic ion loss.

7. Excitation of marginal RWM

In this section, the additional interaction between the EWM-triggered ELM and the RWM is introduced. It is observed that the EWM-triggered ELM seemed to excite the stable RWM.

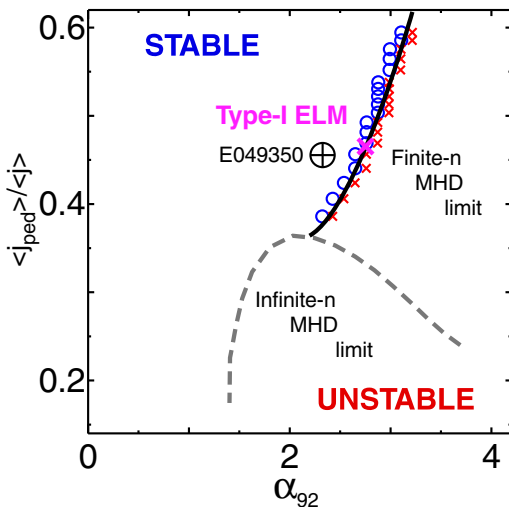


Fig. 12: j - α diagram for just before type-I ELM at $t \simeq 5.975$ s of E049350.

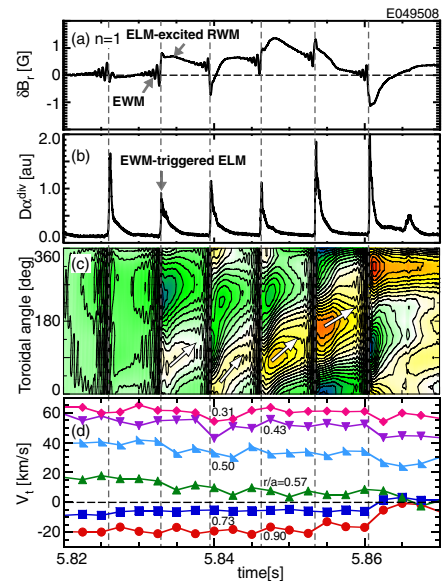


Fig. 13: Time evolutions of (a) $n = 1$ magnetic perturbation, (b) D_{α} emission at the divertor region, (c) toroidal mode structure and (d) toroidal rotations.

In Fig. 13(a) and (b), the time evolution of $n = 1$ magnetic perturbation and D_{α}^{div} are shown. Just after each EWM-triggered ELM, the $n = 1$ magnetic field repeatedly appears. Figure 13(c) shows a contour plot of toroidal structure of the magnetic perturbation. As seen, the excited $n = 1$ response is slowly rotating in the toroidal direction. From the mode structure and time scale, the response is considered to be the stable RWM close to the stability limit. Figure 13(d) shows the time evolution of plasma rotations. Just after the ELM the plasma rotation was decreased. This phenomenon is thought to be the so-called resonant field amplification (RFA) [6]. It has been reported that stable RWM can respond by an application of external fields [7]. From the decay of the excited RWM, the damping rate and mode frequency can be estimated based on an impulse response. Actually, the mode frequency is about 40 Hz, which is consistent with the RWM time scale. The damping is about twice the mode frequency, that is over damping. The observed phenomenon is thought to be a plasma response indicating that the RWM is marginal by the ELM impact.

8. Summary

We have reported the interactions of MHD events in the JT-60U high- β_N plasmas. In the ELMy H-mode with high- β_N plasmas, it is observed that the EWM triggers the ELM. The EWM-triggered ELM has a higher frequency and less energy loss than those of the type-I ELM. Actually, it is observed that the affected region of the EWM-triggered ELM is smaller than that of the type-I ELM. The trigger of the ELM by the EWM occurs as the EWM has a large amplitude. In the SOL region, several measurements indicates ion losses synchronized with an EWM perturbation. Namely, the ion losses enhanced as the EWM amplitude increases. However, whether an EWM can trigger an ELM is not determined by the EWM amplitude. The mechanism that the EWM can trigger the ELM is discussed based on the edge stability diagram calculated by the MARG2D. From the calculation, the edge stability of the discharges are located close to the MHD limit. This indicates the ion losses are possible to increase pedestal pressure gradient as an additional effect, and then trigger an ELM. Whether an EWM can trigger an ELM seems to be determined by the competition between a distance from the MHD boundary and additional pressure of ion losses due to an EWM. Another interaction that the EWM-triggered ELM excited an marginal RWM is observed. Just after the EWM-triggered ELM, an $n = 1$ distortion appears and then decays soon. It is considered that an impact of the induced ELM can excite the marginally stable RWM.

References

- [1] G. Matsunaga et al., *Phys. Rev. Lett.* **103**, 045001 (2009).
- [2] G. Matsunaga et al., *Nuclear Fusion* **50**, 084003 (2010).
- [3] M. Okabayashi et al, *Nuclear Fusion* **49**, 125003 (2009).
- [4] S. Tokuda and T. Watanabe, *Phys. Plasmas* **6**, 3012 (1999).
- [5] N. Aiba et al., *Comput. Phys. Commun.* **175**, 269-289 (2006).
- [6] A. H. Boozer, *Phys. Rev. Lett.* **86**, 5059 (2001).
- [7] H. Reimerdes et al., *Phys. Rev. Lett.* **93**, 135002 (2004).